



On a class of three-phase checkerboards with unusual effective properties

Sur une classe d'échiquiers à trois phases aux propriétés effectives singulières

Richard V. Craster^a, Sébastien Guenneau^{b,*}, Julius Kaplunov^c, Evgeniya Nolde^c

^a Department of Mathematics, Imperial College London, London SW7-2AZ, UK

^b Institut Fresnel, UMR CNRS 6133, University of Aix-Marseille, 13000 Marseille, France

^c Department of Mathematical Sciences, Brunel University, Uxbridge, Middlesex, UB8 3PH, UK

ARTICLE INFO

Article history:

Received 10 December 2010

Accepted after revision 11 March 2011

Available online 20 May 2011

Keywords:

Waves

Homogenization

Negative refraction

Acoustic band

Mots-clés :

Ondes

Homogénéisation

Réfraction négative

Bande acoustique

ABSTRACT

We examine the band spectrum, and associated Floquet–Bloch eigensolutions, arising in a class of three-phase periodic checkerboards. On a periodic cell $[-1, 1]^2$, the refractive index, n , is defined by $n^2 = 1 + g_1(x_1) + g_2(x_2)$ with $g_i(x_i) = r^2$ for $0 \leq x_i < 1$, and $g_i(x_i) = 0$ for $-1 \leq x_i < 0$ where r^2 is constant. We find that for $r^2 > -1$ the lowest frequency branch goes through origin with linear behaviour, which leads to effective properties encountered in most periodic structures. However, the case whereby $r^2 = -1$ is very unusual, as the frequency λ behaves like \sqrt{k} near the origin, where k is the wavenumber. Finally, when $r^2 < -1$, the lowest branch does not pass through the origin and a zero-frequency band gap opens up. In the last two cases, effective medium theory breaks down even in the quasi-static limit, while the high-frequency homogenization [R.V. Craster, J. Kaplunov, A.V. Pichugin, High-frequency homogenization for periodic media, Proc. R. Soc. Lond. Ser. A 466 (2010) 2341–2362] neatly captures the detailed features of band diagrams.

© 2011 Published by Elsevier Masson SAS on behalf of Académie des sciences.

R É S U M É

Nous étudions le spectre de bande associé aux modes de Floquet–Bloch dans une classe d'échiquiers périodiques. Sur une cellule de base $[-1, 1]^2$, l'indice de réfraction, n , est défini par $n^2 = 1 + g_1(x_1) + g_2(x_2)$ où $g_i(x_i) = r^2$ (une constante) pour $0 \leq x_i < 1$, et $g_i(x_i) = 0$ pour $-1 \leq x_i < 0$. Pour $r^2 > -1$, la première bande passe par l'origine avec un comportement linéaire, ce qui conduit à des propriétés effectives rencontrées dans la plupart des structures périodiques. En revanche, le cas $r^2 = -1$ est moins ordinaire, puisque la bande de fréquences acoustiques λ se comporte comme \sqrt{k} au voisinage de l'origine, avec k le nombre d'onde. Finalement, quand $r^2 < -1$, la bande acoustique disparaît : la première bande ne passe plus par l'origine et une bande interdite à fréquence nulle apparaît. Dans ces deux derniers cas de figure, la théorie des milieux effectifs ne s'applique pas, alors que la théorie d'homogénéisation hautes fréquences [R.V. Craster, J. Kaplunov, A.V. Pichugin, High-frequency homogenization for periodic media, Proc. R. Soc. Lond. Ser. A 466 (2010) 2341–2362] reproduit avec précision les diagrammes de bandes.

© 2011 Published by Elsevier Masson SAS on behalf of Académie des sciences.

* Corresponding author.

E-mail addresses: r.craster@imperial.ac.uk (R.V. Craster), sebastien.guenneau@fresnel.fr (S. Guenneau), julius.kaplunov@brunel.ac.uk (J. Kaplunov), evgeniya.nolde@brunel.ac.uk (E. Nolde).

Version française abrégée

Nous considérons un échiquier périodique dont la géométrie est décrite dans la Fig. 1. Les ondes optiques ou acoustiques qui s'y propagent sont solutions de l'équation de Helmholtz (1) dans les cases homogènes occupées par des matériaux ou fluides isotropes dont le carré de l'indice de réfraction est positif, nul, ou négatif. Par ailleurs, des conditions classiques de continuité de la composante tangentielle du champ électromagnétique (ou du champ de déplacement/pression et de sa dérivée normale) sont imposées aux interfaces entre les différents matériaux/fluides de la cellule élémentaire et des conditions de Floquet–Bloch sur les bords opposés de celle-ci. Dans le cadre de la théorie d'homogénéisation hautes fréquences développée dans [1], nous nous intéressons plus particulièrement au cas où les conditions de Floquet–Bloch se réduisent à des conditions périodiques ou anti-périodiques, ce qui permet de déduire l'équation homogénéisée (4) qui conduit à une estimation fine des courbes de dispersion à travers la fréquence effective (5), pour des nombres d'onde au voisinage des points A , B et C de la zone de Brillouin, cf. Fig. 1. Il s'avère que l'on peut même déduire les relations de dispersion analytiquement dans le cas d'échiquiers à trois phases, données par (7) et (6).

Grâce à ces approches de type homogénéisation hautes fréquences [1], et Krönig–Penney [2], nous mettons en exergue trois types de comportements effectifs pour des ondes se propageant dans de tels échiquiers aux basses fréquences : ordinaire de type cristal photonique ($r^2 > -1$: bande acoustique linéaire à l'origine, voir Figs. 2(a) et 4(a)), singulier de type cristal plasmonique ($r^2 = -1$: bande acoustique non linéaire à l'origine, voir Fig. 3(a)) et de type métamatériaux ($r^2 < -1$: perte de bande acoustique i.e. bande interdite à fréquence nulle, voir Fig. 3(b)).

Nous concluons notre étude par une application de type lentille échiquier par réfraction négative [3,4] quand $r^2 > -1$, avec l'image d'un point source à la fréquence donnée par l'estimation (8), voir Fig. 4(b). Nous notons que dans ce cas de figure, la réfraction négative résulte d'une vitesse de groupe négative pour des ondes se propageant suivant la direction CA du réseau de Brillouin, voir Fig. 4(a), ce qui induit une rotation des cellules de base de l'échiquier d'un angle de 45 degrés, comme il transparait en Fig. 4(b). Géométriquement, la fréquence donnée par (8) correspond à l'intersection de la bande acoustique suivant CA et de la droite de pente -1 issue de A (en traits pointillés), généralement appelée cône de lumière dans la littérature optique (qui correspond à la dispersion d'une onde optique ou acoustique en milieu homogène) [5,6]. Des effets de focalisation similaires peuvent-être obtenus dans des structures périodiques pour les ondes de pression dans les fluides ou les vagues à la surface d'un liquide [7–10].

1. Introduction: Beyond effective medium theory with high-frequency homogenization

Negative refraction is an emerging field in photonics introduced by Victor Veselago in the late 1960's [3], with renewed interest following the controversial claim of John Pendry that negative refraction makes a flat lens with unlimited resolution possible [4]. The quest for this superlens has fuelled research in structured photonic materials during the last decade. These composites are known as photonic crystals when the wavelength of light is of the same order as the typical heterogeneity size (Bragg frequency regime), and metamaterials when the wavelength is much larger (low-frequency homogenization regime). The propagation of waves with anti-parallel group and phase velocities, an essential ingredient for negative refraction, was discussed in the late 1940's by Léon Brillouin [11].

In order to investigate the properties of photonic crystals, we consider the Helmholtz equation (1) in a periodic medium. This equation could, with appropriate notational and linguistic changes, hold for acoustic, electromagnetic, water or out-of-plane elastic waves and so encompasses many possible physical applications. We solve

$$\frac{\partial^2 u}{\partial x_1^2} + \frac{\partial^2 u}{\partial x_2^2} + \lambda^2 [1 + g_1(x_1) + g_2(x_2)] u = 0 \quad (1)$$

for $u(x_1, x_2)$ on the square $-1 < x_1, x_2 \leq 1$, where λ^2 is the frequency squared. In the case of a three-phase checkerboard with a square cell as shown in Fig. 1, $g_i(x_i)$ is taken to be the piecewise constant

$$g_i(x_i) = r^2 \quad \text{for } 0 \leq x_i < 1, \quad \text{and} \quad g_i(x_i) = 0 \quad \text{for } -1 \leq x_i < 0 \quad (2)$$

We note that in the context of optics, the unknown u in (1) stands for the longitudinal component of the electric field E_z and λ^2 is associated with ω^2/c^2 whereby ω is the electromagnetic wave frequency and c is the speed of light in vacuum. Moreover, $\varepsilon_r \mu_0 = 1 + g_1(x_1) + g_2(x_2)$ where $\mu_0 = 1$ and ε_r are the relative permeability and permittivity of the dielectric (non-magnetic) medium, respectively.

For waves through an infinite, perfect, doubly periodic checkerboard one can invoke Bloch's theorem [11] and simply consider the square cell with quasi-periodic Bloch boundary conditions applied to the edges:

$$\begin{aligned} u(1, x_2) &= e^{ik_1} u(-1, x_2), & u_{x_1}(1, x_2) &= e^{ik_1} u_{x_1}(-1, x_2) \\ u(x_1, 1) &= e^{ik_2} u(x_1, -1), & u_{x_2}(x_1, 1) &= e^{ik_2} u_{x_2}(x_1, -1) \end{aligned} \quad (3)$$

that involves the Bloch wave-vector $\kappa = (\kappa_1, \kappa_2)$ characterizing the phase-shift as one moves from one cell to the next. There is also continuity of u , u_{x_1} , u_{x_2} along $x_1 = 0$ and $x_2 = 0$. This Bloch problem is solved explicitly and dispersion relations that link the frequency and Bloch wavenumber are deduced; as is well-known in solid state physics [11] only a limited range of

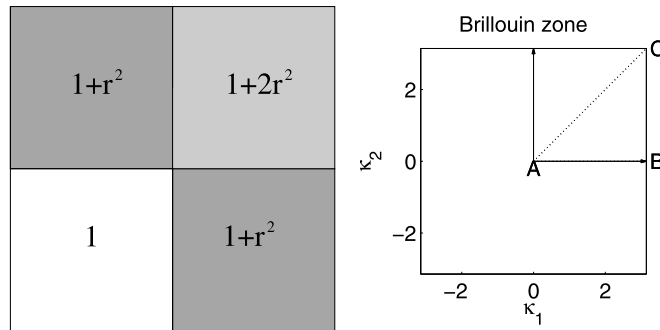


Fig. 1. Left: A single cell for the checkerboard geometry, for piecewise constant media. Right: The reciprocal Brillouin lattice in wavenumber, $\kappa = (\kappa_1, \kappa_2)$, space.

wavenumbers need be considered, namely the wavenumbers along the triangle shown in the reciprocal Brillouin lattice of Fig. 1 and these form the irreducible Brillouin zone. The dispersion curves reported in Figs. 3–4 illustrate several interesting features: stop-bands for which wave propagation is not possible, and regions of flat dispersion curves for which the group velocity is zero and features of slow sound or light occur. In this paper, we focus our attention to the lowest curves, associated with averaged properties of the checkerboards, and discuss the extension of existing effective theories to higher frequencies.

Conventional homogenization is widely assumed to be ineffective for modeling photonic crystals as it is limited to low frequencies when the wavelength is long relative to the microstructural lengthscales. Here the recently developed high-frequency homogenization theory [1], which is free of the conventional limitations, is used to generate effective partial differential equations on a macroscale, that have the microscale embedded within them through averaged quantities. We focus our attention on periodic checkerboards, some of them with sign-shifting coefficients [20,22]: the latter are known to support a host of surface plasmons associated with highly resonant features less than conducive for any effective theory. Our aim is actually to push the newly introduced high-frequency homogenization beyond its limits.

At leading order, the field $u(\mathbf{x})$ propagating inside the periodic checkerboard can be represented as $U(\xi)f(\mathbf{X})$ where ξ and \mathbf{X} are the short- and long-scales [1]. The function U represents the local short-scale solution at a specific standing wave frequency, λ_0 (which is in the high-frequency regime), and f the long-scale variation. Ultimately a homogenized PDE emerges for f entirely on the macroscale [1]

$$T_{ij} \frac{\partial^2 f}{\partial X_i \partial X_j} + \frac{(\lambda^2 - \lambda_0^2)}{\epsilon^2} f = 0 \tag{4}$$

where the spatially constant tensor T_{ij} incorporates the short-scale information associated with the standing wave frequency λ_0 ; λ is the full frequency and there is summation over repeated suffices. For the checkerboard, the general formulae for the coefficients T_{ij} are expressed in terms of double integrals over the cell, as in [1], and can be reduced to completely explicit trigonometric expressions.

The PDE can be augmented by additional terms if there is material variation leading to localized defect modes [13] or localized forcing [14]. The PDE (4) can then be utilized for, say, Bloch waves where $f \sim \exp(i\mathbf{k} \cdot \mathbf{X}/2)$, to find local dispersion relations

$$\lambda \sim \lambda_0 \left(1 + \epsilon^2 \frac{T_{ij} k_i k_j}{8\lambda_0^2} \right) \tag{5}$$

valid near the standing wave frequency λ_0 ; this formula is explicitly for those periodic-periodic standing waves at wavenumber A and almost identical formulae hold for the other standing waves. Thus, the constants T_{ij} , once identified, completely encapsulate the effect of the microstructure on the dispersion properties of the system; the disparity of scales is represented by ϵ which is assumed positive and $\ll 1$. Some typical values of the tensor T_{ij} are given for the cases $r^2 = -1$ and -0.9 in Table 1 and $r^2 = -2$ in Table 2. One should note that in some cases the diagonal entries, are identical (effective isotropic parameters), different (anisotropic parameters) and even of opposite signs (a hallmark of anomalous dispersion).

2. An exact dispersion relation for a class of three-phase checkerboards

We have first investigated the dispersion curves associated with three-phase periodic checkerboards using the finite element software COMSOL Multiphysics. However, the convergence of the numerical algorithm can be hazardous, due to sign-shifting coefficients [22]. Thankfully, the Bloch problem for such checkerboards can be solved analytically and this provides probably the only non-trivial two-dimensional structure with an exact solution; it is a natural generalization of the classical Kronig–Penney [2] one-dimensional piecewise constant periodic medium. The dispersion relation follows from

Table 1

The standing wave frequencies, λ , the μ and the corresponding T_{11} and T_{22} for the lowest three dispersion curves for $r^2 = -1$ and $r^2 = -0.9$.

$r^2 = -1$					$r^2 = -0.9$				
	λ	μ	T_{11}	T_{22}		λ	μ	T_{11}	T_{22}
A	0	0	N/A	N/A	A	0	0	N/A	N/A
A	4.801	2.605	-2.907	0.195	A	4.678	2.544	-4.436	0.278
A	4.801	2.605i	0.195	-2.907	A	4.678	2.544i	0.278	-4.436
C	2.652	0	-1.813	-1.813	C	2.6086	0	-2.1778	-2.1778
C	4.519	2.345	2.951	-0.380	C	4.263	2.1596	4.079	-0.678
C	4.519	2.345i	-0.380	2.951	C	4.263	2.1596i	-0.678	4.079
B	2.336	0.767i	-3.445	1.394	B	2.2473	0.8165i	-4.3226	1.4607
B	4.477	2.350i	3.215	0.384	B	4.1814	2.1623i	4.7095	0.6936
B	4.821	2.595	-0.199	-2.774	B	4.708	2.530	-0.2883	-4.1548

Table 2

Values of λ and the corresponding μ at the wavenumbers for standing waves with the associated values of T_{11} and T_{22} for the lowest dispersion curve for $r^2 = -2$.

$r^2 = -2$				
	λ	μ	T_{11}	T_{22}
A	2.8898	0	0.4519	0.4519
C	3.0217	0	-0.3412	-0.3412
B	2.9632	0.3524	-0.41	0.3596

setting $u(x_1, x_2) = Q_1(x_1)Q_2(x_2)$ in the governing equation (1). From the piecewise constant function (2), and from the Bloch conditions (3), the following coupled equations emerge [12]

$$2\gamma_i\beta_i(\cos\kappa_i - \cos\gamma_i\cos\beta_i) + (\beta_i^2 + \gamma_i^2)\sin\gamma_i\sin\beta_i = 0 \tag{6}$$

for $i = 1, 2$. These are dispersion relations for λ^2, μ^2 (the latter is a separation constant) in terms of κ_1, κ_2 ; the parameters γ_i, β_i act to couple the equations as

$$\beta_i^2 = \lambda^2/2 \mp \mu^2, \quad \gamma_i^2 = \lambda^2(1/2 + r^2) \mp \mu^2 \tag{7}$$

for $i = 1, 2$ with the minus, plus signs for $i = 1, 2$ respectively. This two variable dispersion relation is solved via matrix Newton iteration. For the exact solution found in this section, one finds λ, μ explicitly and some sample eigenvalues are given in Table 1. Notably some frequencies, λ , have two associated μ values, one real and one imaginary and these correspond to degenerate cases where the dispersion curves touch.

3. Illustrative electromagnetic paradigms whereby effective medium theory fails

Effective properties of periodic checkerboards are of particular mathematical interest, and their study goes back a long way, with the seminal paper by Keller [15] for two-phase checkerboards, and those of Mortola–Steffe [16], Craster–Obnosov [17] and Milton [18] for four-phase checkerboards. Physicists have further analyzed the effective properties of two-phase checkerboards with continuously varying parameters in the context of photonic crystals [19]. In this note, we investigate the case of three-phase checkerboards with negative and vanishing refractive index squared (when r^2 takes values lower or equal than -1). Such a study is motivated by the fabrication of nano-scale gold and silver checkerboards whose cells alternate positive and negative refractive index squared media in the visible range of frequencies. Potential applications lie in extra-ordinary transmission of light through the sub-wavelength aperture holes in such checkerboards, and tremendously enhanced local density of states for light confinement [20]. These physical phenomena are underpinned by the effective properties of such checkerboards. Hence, an adequate homogenization model for such structures is of pressing importance.

We start with the canonical case of a three-phase checkerboard with $r^2 = 1$. Dispersion diagrams reported in Fig. 2(a) compare the solution from the exact dispersion relations (dashed lines) with those from the high-frequency homogenization approach (solid lines). We note that most curves are well approximated by the asymptotics, and in particular the optical band (second curve) which cannot be captured by standard homogenization techniques. The negative slope of the optical band along the AC direction leads to a negative group velocity associated with all-angle-negative-refraction, see [5,6] for applications in optics and [7–10] in acoustics.

We now explore the case of a checkerboard with $r^2 = -0.9, -1$ and 1 . A close-up view on a log–log scale of the acoustic band in Fig. 2(b) reveals that the long wave low-frequency limit for $r^2 = -0.9$ differs substantially from that when $r^2 = -1$. For $r^2 = -1$ the usual effective medium result that frequency is linearly related to wavenumber no longer holds; a different asymptotic relation arises, see Fig. 2(b) where $\lambda \sim 6^{1/4}\sqrt{|\kappa|}$. The change in behavior occurs due to a degeneracy in the asymptotics for $r^2 = -1$, although they still work and the new relation emerges.

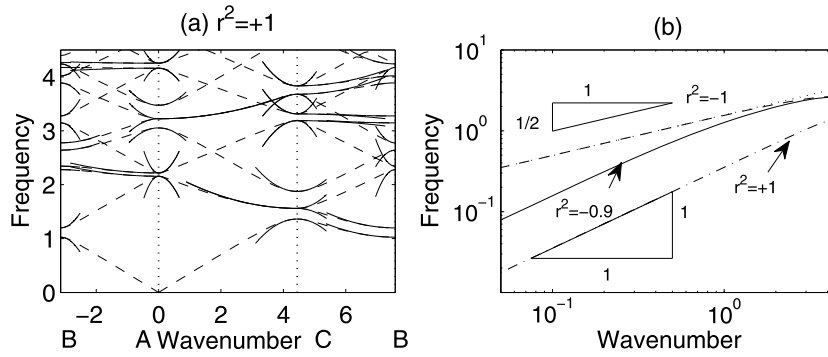


Fig. 2. Dispersion diagrams for $r^2 = 1$ and local behavior of the acoustic band for vanishing wavenumbers when $r^2 = -1, -0.9$ and 1 . Panel (a) shows the dispersion curves from the exact solutions (dashed curves) that are visually close to those from the asymptotic estimates (solid curves). Panel (b) shows the lowest dispersion curve along AC on log-log axes. The dashed line is for $r^2 = -1$ and its slope is $1/2$, the superimposed dots are $\lambda \sim 6^{1/4} \sqrt{|\kappa|}$. The solid line for $r^2 = -0.9$ and the lowest line for $r^2 = 1$ show the usual $\lambda \sim |\kappa|$ linear behavior.

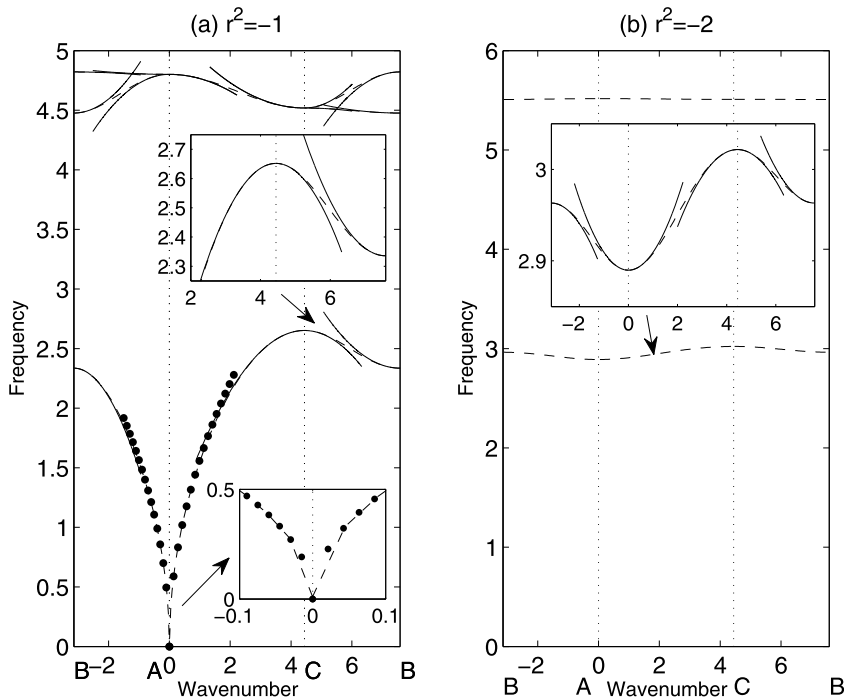


Fig. 3. Dispersion diagrams for $r^2 = -1$ (a) and $r^2 = -2$ (b). Panel (a) shows the lowest three exact dispersion curves from the explicit dispersion relations and the asymptotic dispersion curves with the behavior at the lowest curve that touches the origin shown dotted. The lower inset shows the detail near the origin comparing the exact (dashed) and asymptotic (dotted) solutions. The upper inset shows a similar comparison (asymptotics given by the solid line) for the lowest curve near wavenumber position C. Panel (b) shows that there is no acoustic band and that the dispersion curves are nearly flat. The inset shows an enhanced view of the lowest dispersion branch with the numerics (dashed) shown together with asymptotics (solid).

The dispersion diagrams reported in Fig. 3 compare the solution from the exact dispersion relations with those from the asymptotics when $r^2 = -1$ and -2 . Fig. 3(a) clearly demonstrates the superiority of the high-frequency homogenization approach which reproduces very precisely the acoustic and optical branches, thereby extending classical homogenization to the stop band (Bragg) regime of frequencies. Moreover, the region where the lowest branch cuts the origin, the long wave low-frequency regime, is no longer linear and asymptotics of the dispersion relation show that the local behavior is that $\lambda \sim 6^{1/4} |\kappa|^{1/2}$ (cf. also Fig. 2(b)). The insets show details of the asymptotics versus the exact solution. Fig. 3(b) shows the case of a checkerboard with $r^2 = -2$; the acoustic band is lost for $r^2 < -1$, which is reminiscent of singular problems in homogenization of periodic arrays of infinitely conducting fibres in transverse electric polarization (modeled with Dirichlet boundary conditions) [21]. In the present case, we do not consider Dirichlet conditions (corresponding to hard walls in acoustics) but we rather have sign-shifting conditions across some interfaces [22]. It is clear that effective medium theory breaks down, however the high-frequency homogenization approach captures the fine features of the nearly

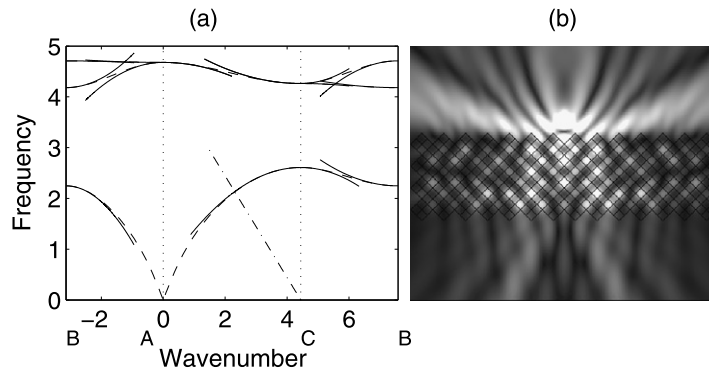


Fig. 4. Dispersion diagrams for $r^2 = -0.9$. Panel (a) shows the dispersion curves that are visually close to those for $r^2 = -1$ however, the behavior near A for low frequency is asymptotically different between these cases. The dot-dash line is the light-line for waves impinging upon the rotated checkerboard. Panel (b) shows the absolute value of field u (e.g. the transverse electric field in optics, or the pressure field in acoustics) solution of the Helmholtz equation (1) for a harmonic point source at frequency $\lambda = 2.1$ above a finite size checkerboard for $r^2 = -0.9$ with each cell rotated by an angle $\pi/4$; it displays an image below the checkerboard in accordance with the Snell-Descartes law for a negative refractive index. We note that the resolution of the image is about half the wavelength along the x -axis and twice the wavelength along the y -axis (elongated image). This means the focused signal is constrained within an area no smaller than a wavelength squared (i.e. no sub-wavelength resolution).

flat dispersion curves, see the inset to Fig. 3(b), which are associated with slow waves, another topical subject in photonics (with applications in delay lines and highly-directive antennas).

We finally wish to explore in more details the spectrum for the case of a checkerboard with $r^2 = -0.9$. Fig. 4(a) looks visually similar to Fig. 3(a); however, a closer view on a log-log scale (see Fig. 2(b)) of the acoustic band reveals that the long wave low-frequency limit differs from that when $r^2 = -1$. For $r^2 = -0.9$ one gets the usual effective medium result with frequency linearly related to wavenumber however for $r^2 = -1$ the effective medium theory no longer holds and a different asymptotic relation holds ($\lambda \sim 6^{1/4} |\kappa|^{1/2}$); we further observe that the high-frequency homogenization approach (dotted line) captures the fine features of this curve (dashed line).

Importantly, Fig. 4(a) also shows the light-line emerging from C relevant for waves impinging upon a checkerboard structure rotated through $\pi/4$. Notably the light-line crosses the lowest dispersion curve in such a way that their group velocities are opposite and therefore one can induce negative refraction at this frequency. The asymptotic theory explicitly identifies this frequency as

$$\lambda = \lambda_0 / \sqrt{1 - T/4} \quad (8)$$

where $T_{11} = T_{22} = T$ for that case. The estimate is that $\lambda \sim 2.1$ and computations for this are shown in Fig. 4.

4. Conclusions

We have investigated the Bloch spectrum of periodic, three-phase, checkerboards. While in [12] we apply the high-frequency homogenization theory [1] to localization and lensing effects in dielectric photonic checkerboards, the focus has been here on special cases in which the refractive index squared (i.e. the relative permittivity in the context of optics) in homogeneous cells can take vanishing and/or negative values (which is a good model for Drude metals, e.g. gold or silver), and we have found that anomalous dispersion effects of waves are possible, including acoustic bands with non-linear features for vanishing wavenumbers, zero frequency stop bands, and nearly flat dispersion curves. The last two items are known to be respectively associated with singularly perturbed problems in electromagnetism that cannot be homogenized in a conventional way [21], as no wave is allowed to propagate in the periodic structure at low frequencies, and slow waves, whereby delay lines can be achieved.

Acknowledgements

The authors gratefully acknowledge the support of the UK EPSRC through Grant number EP/H021302. R.V.C. thanks NSERC Canada for their support through the Discovery Grant scheme.

References

- [1] R.V. Craster, J. Kaplunov, A.V. Pichugin, High-frequency homogenization for periodic media, Proc. R. Soc. Lond. Ser. A 466 (2010) 2341–2362.
- [2] R.L. Kronig, W.G. Penney, Quantum mechanics in crystals lattices, Proc. R. Soc. Lond. 130 (1931) 499–531.
- [3] V.G. Veselago, The electrodynamics of substances with simultaneously negative value of ϵ and μ , Sov. Phys. Usp. 10 (1968) 509–514.
- [4] J.B. Pendry, Negative refraction makes a perfect lens, Phys. Rev. Lett. 86 (2000) 3966.
- [5] B. Gralak, S. Enoch, G. Tayeb, Anomalous refractive properties of photonic crystals, J. Opt. Soc. Am. A 17 (2000) 1012.
- [6] C. Luo, S.G. Johnson, J.D. Joannopoulos, All-angle negative refraction without negative effective index, Phys. Rev. B 65 (2002) 201104.

- [7] P. McIver, Water-wave propagation through an infinite array of cylindrical structures, *J. Fluid Mech.* 424 (2000) 101–125.
- [8] X. Hu, Y. Schu, X. Liu, R. Fu, J. Zi, Superlensing effect in liquid surface waves, *Phys. Rev. E* 69 (2004) 030201.
- [9] Z. Shu, L. Yin, N. Fang, Focusing ultrasound with acoustic metamaterial network, *Phys. Rev. Lett.* 102 (19) (2009) 194301.
- [10] M. Farhat, S. Guenneau, S. Enoch, A.B. Movchan, All-angle-negative-refraction and ultra-refraction for liquid surface waves in 2-D phononic crystals, *J. Comput. Appl. Math.* 234 (2010) 2011–2019.
- [11] L. Brillouin, *Wave Propagation in Periodic Structures*, McGraw-Hill, 1946.
- [12] R.V. Craster, J. Kaplunov, E. Nolde, S. Guenneau, High-frequency homogenization for checkerboard structures: Defect modes, ultrarefraction, and all-angle negative refraction, *J. Opt. Soc. Am. A* 28 (6) (2011) 1032–1040.
- [13] R.V. Craster, J. Kaplunov, J. Postnova, High frequency asymptotics, homogenization and localization for lattices, *QJMAM* 63 (2010) 497–519.
- [14] E. Nolde, R.V. Craster, J. Kaplunov, High frequency homogenization for structural mechanics, *J. Mech. Phys. Solids* 59 (2010) 651–671.
- [15] J.B. Keller, A theorem on the conductivity of a composite medium, *J. Math. Phys.* 5 (1964) 548.
- [16] S. Mortola, S. Steffe, A two-dimensional homogenization problem, *Atti Accad. Naz. Lincei Rend. Cl. Sci. Fis. Mat. Natur.* 78 (1985) 77.
- [17] R.V. Craster, Y.V. Obnosov, Four phase checkerboard composites, *SIAM J. Appl. Math.* 61 (2001) 1839–1856.
- [18] G.W. Milton, Proof of a conjecture on the conductivity of checkerboards, *J. Math. Phys.* 42 (2001) 4873–4882.
- [19] F. Zolla, S. Guenneau, Duality relation for the Maxwell system, *Phys. Rev. E* 67 (2003) 026610.
- [20] S. Guenneau, S.A. Ramakrishna, Negative refractive index, perfect lenses and checkerboards: Trapping and imaging effects in folded optical spaces, *C. R. Physique* 10 (2009) 352–378.
- [21] C.G. Poulton, L.C. Botten, R.C. McPhedran, N.A.P. Nicorovici, A.B. Movchan, Non-commuting limits in electromagnetic scattering: asymptotic analysis for an array of highly conducting inclusions, *SIAM J. Appl. Math.* 61 (2001) 1706–1730.
- [22] A.-S. Bonnet-BenDhia, P. Ciarlet Jr., C.M. Zwolf, Time harmonic wave diffraction problems in materials with sign-shifting coefficients, *J. Comput. Appl. Math.* 234 (6) (2010) 1912–1919.